

"SMILE": A SELF MAGNETICALLY INSULATED TRANSMISSION LINE ADDER FOR THE 8-STAGE RADLAC II ACCELERATOR*

M. G. MAZARAKIS, J. W. POUEY, S. L. SHOPE, C. A. FROST,
B. N. TURMAN, J. J. RAMIREZ, and K. R. PRESTWICH
Sandia National Laboratories
P. O. Box 5800
Albuquerque, NM 87185

P. J. PANKUCH
EG&G Special Projects
2450 Alamo Avenue SE, P. O. Box 9100
Albuquerque, NM 87119

Abstract

The RADLAC II Self Magnetically Insulated Transmission Line "SMILE" is a coaxial wave guide structure that is composed of two regions: a) a 9.5-m voltage adder and b) a 3-m long extension section. The adder section provides for the addition of the input voltages from the individual water-dielectric pulse forming line feeds. The extension section isolates the adder from the magnetically immersed foilless diode electron source load and efficiently transports the pulsed power out from the deionized water tank of the device. The SMILE modification of the RADLAC II accelerator enabled us to produce high quality beams of up to 14 MV, 100 kA. The design and the experimental evaluation of SMILE will be presented and compared with numerical simulation predictions.

Introduction

The RADLAC II accelerator in its original configuration was an electron induction linear accelerator designed to produce ~100 kA, 16 MeV electron beams. The beam was produced by a magnetically immersed foilless diode located at the lower voltage end of the device (4-MV injector). It was then transported magnetically through a vacuum pipe 5 cm in diameter and further accelerated through the remaining six postaccelerating gaps of 2-MV accelerating voltage each. A magnetic transport system composed of 50 individual solenoids each of 20-kG field strength was utilized. The 100-kA electron beam was effectuating the voltage addition of each gap by increasing the kinetic energy of its electrons by an increment equal to the potential differential of each gap.

By now, it is well known in the accelerator community that high current electron induction accelerators have difficulties—they are particularly prone to beam instabilities due to beam-accelerating gap interactions, beam-accelerating cavity interactions, beam-vacuum pipe interactions, etc. When these instabilities are coupled with misalignment and non-uniformity of the magnetic transport system, the situation becomes worse and the beam can strike the vacuum pipe wall before its acceleration is complete. While the RADLAC II beam handling system was designed to avoid all the known beam instabilities¹, provisions were not made at that time for the degree of precision which we now know is necessary in aligning the vacuum beam pipe and the solenoidal magnets. In addition, poor field uniformity and a lack of structural integrity in the magnets made the beam's acceleration and transport through the machine a very difficult task.

The SMILE modification of RADLAC II and its subsequent successful operation proves that a high final impedance (~150 ohm) induction linac does not necessarily need a beam in order to add up the potential energy of the voltage feeds. A central conductor² that goes through all the accelerating cavities (feeds) can do the job much better and more cheaply, avoiding fatal beam instabilities and expensive and sophisticated transport systems. After all, since in an induction linac the beam is the secondary of a one to one transformer, we may as well provide the "secondary" conductor along or near the surface of which the electrons can flow.

SMILE did precisely that for the RADLAC II accelerator. Of course the central conductor, "secondary," had to be designed according to Creedon's prescriptions³ in order to provide self-magnetic insulation for the moving electrons. In the next three sections, we present the SMILE design, the numerical simulations validating it, and RADLAC II's performance with SMILE.

The SMILE Design

Before making a total transition to a central conductor, we gradually substituted sections of the beam transport and accelerating system with self-magnetically insulated transmission line voltage adders (MITL). The beam was produced at the end of the adder in a foilless diode configuration and then accelerated and magnetically transported through the remaining part of the device. We successfully designed and operated a two-feed (4 MV) and a four-feed (8 MV) self-magnetically insulated transmission line injector.^{4, 5} Finally we removed all of the old transport system and installed SMILE, which extended the MITL voltage adder to the end of the device. The design is similar to that of the HELIA⁶, HERMES III⁷, and SABRE^{8, 9} accelerators and was done using the Creedon formalism³.

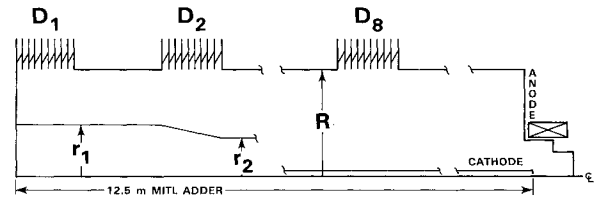


Fig. 1: Schematic cross section of the SMILE adder system.

The SMILE design is based on a pulse forming line-fed self-magnetically insulated transmission line (MITL) system which performs the series addition of voltage pulses from eight source modules (feeds). The cathode geometry is shown in Figure 1. It is preferred over a continuous taper for the following reasons: it is easier and cheaper to manufacture, the constant radius segments provide constant vacuum impedance along each MITL segment, and the impedance increases gradually at each successive voltage feed with a rate of increase which follows the voltage axial gradient along the feed. The latter assures constant current flow over the entire length of SMILE.

The vacuum impedance of each section i of SMILE depends only on the dimensions of Figure 1 and can be easily calculated from the following expression:

$$Z_i = 60 \ln (R/r_i) [\Omega]; i = 1, 2, \dots, 8 \quad (1)$$

where $R = 19$ cm and is the anode inner radius and r_i is the radius of the i -th cathode segment. The selection of the radius r_i of each cylindrical section was done in a fashion to provide constant operating load impedance for all of the pulse forming line feeds of RADLAC II. (Optimum cathode radius, TABLE I).

*Supported by the U.S. DOE Contract DE-AC04-76DP00789.

Report Documentation Page				Form Approved OMB No. 0704-0188	
Public reporting burden for the collection of information is estimated to average 1 hour per response, including the time for reviewing instructions, searching existing data sources, gathering and maintaining the data needed, and completing and reviewing the collection of information. Send comments regarding this burden estimate or any other aspect of this collection of information, including suggestions for reducing this burden, to Washington Headquarters Services, Directorate for Information Operations and Reports, 1215 Jefferson Davis Highway, Suite 1204, Arlington VA 22202-4302. Respondents should be aware that notwithstanding any other provision of law, no person shall be subject to a penalty for failing to comply with a collection of information if it does not display a currently valid OMB control number.					
1. REPORT DATE JUN 1991		2. REPORT TYPE N/A		3. DATES COVERED -	
4. TITLE AND SUBTITLE "Smile": A Self Magnetically Insulated Transmission Line Adder For The 8-Stage Radlac II Accelerator				5a. CONTRACT NUMBER	
				5b. GRANT NUMBER	
				5c. PROGRAM ELEMENT NUMBER	
6. AUTHOR(S)				5d. PROJECT NUMBER	
				5e. TASK NUMBER	
				5f. WORK UNIT NUMBER	
7. PERFORMING ORGANIZATION NAME(S) AND ADDRESS(ES) Sandia National Laboratories P. O. Box 5800 Albuquerque, NM 87185				8. PERFORMING ORGANIZATION REPORT NUMBER	
9. SPONSORING/MONITORING AGENCY NAME(S) AND ADDRESS(ES)				10. SPONSOR/MONITOR'S ACRONYM(S)	
				11. SPONSOR/MONITOR'S REPORT NUMBER(S)	
12. DISTRIBUTION/AVAILABILITY STATEMENT Approved for public release, distribution unlimited					
13. SUPPLEMENTARY NOTES See also ADM002371. 2013 IEEE Pulsed Power Conference, Digest of Technical Papers 1976-2013, and Abstracts of the 2013 IEEE International Conference on Plasma Science. Held in San Francisco, CA on 16-21 June 2013. U.S. Government or Federal Purpose Rights License					
14. ABSTRACT The RADLAC II .Self Magnetically Insulated Transmission .Line "SMILE" is a coaxial wave guide structure that is composed of two regions: Â·a) a 9.5-m voltage adder and b) a 3-m long extension section. The adder section provides for the addition of the input voltages from the individual waterdielectric pulse formmg line feeds. The extension section isolates the adder from the magnetically immersed foilless diode electron source load and efficiently transports the pulsed power out from the deionized water tank of the device.					
15. SUBJECT TERMS					
16. SECURITY CLASSIFICATION OF:			17. LIMITATION OF ABSTRACT SAR	18. NUMBER OF PAGES 4	19a. NAME OF RESPONSIBLE PERSON
a. REPORT unclassified	b. ABSTRACT unclassified	c. THIS PAGE unclassified			

Some deviations were allowed at the beginning of the cathode shank where self-magnetic insulation is not that critical and also at the high voltage end for mechanical and construction reasons. (Actual cathode radius, TABLE I).

TABLE I

MITL SEGMENT	SEGMENT VOLTAGE	OPTIMUM CATHODE RADIUS	ACTUAL CATHODE RADIUS	VACUUM IMPEDANCE	OPERATING IMPEDANCE
i	V_i [MV]	r_i [cm]	r_i [cm]	Z_i [Ω]	Z_i [Ω]
1	2.0	13.33	10.2	45.3	30
2	4.0	8.05	7.6	55.0	40
3	6.0	6.30	5.7	80.0	61
4	8.0	3.86	3.5	96.0	80
5	10.0	2.69	2.5	121.0	97
6	12.0	1.90	1.6	149.0	122
7	14.0	1.35	1.3	162.0	135
8	16.0	0.952	1.0	180.0	151

The point design is for 106 kA and assumes equal 2-MV voltages at each insulating stack feed. A MITL operating with conditions similar to SMILE is a "balanced" one. Because of the relatively short voltage pulse (40-ns fwhm) of each feed, the current flow is self limited and, to a large extent, independent of the diode impedance conditions. However, in our design we stayed as close as possible to the constant current conditions all the way to the end of the cathode tip. At first we selected the radius of the cathode tip. The outside wall radius of the anode cylinder was defined by the existing RADLAC II insulating stacks, and the end voltage was assumed to be 16 MV. With these initial parameters and Creedon equations for minimum current flow, I_ℓ , to establish self-limited magnetic insulation:

$$I_\ell = 8500 g \gamma_\ell^3 \ln \left[\gamma_\ell + (\gamma_\ell^2 - 1)^{1/2} \right], \quad (2)$$

$$\gamma_i = \gamma_\ell + (\gamma_\ell^2 - 1)^{3/2} \ln \left[\gamma_\ell + (\gamma_\ell^2 - 1)^{1/2} \right],$$

$$g = [\ln R/r_i]^{-1} \text{ and } \gamma_i = V_i [\text{MV}] / mc^2 + 1,$$

we estimate the cathode radii and operating impedances of the entire SMILE line.

Our main concern was to keep the currents I_ℓ the same. The relativistic factor γ_ℓ is for electrons at the outer boundary of the electron sheath in the minimum current case. It can be approximated by the following formula which is tested to be correct¹⁰ for up to 20 MV adders:

$$\gamma_\ell = \frac{12 \gamma_i^{1/3}}{12 + \ln \left(\frac{\gamma_i}{5.9314} \right)} \quad (3)$$

Table I summarizes SMILE dimensions and design parameters. The cathode electrode was 12.5-m long and was cantilevered from the low voltage end of the accelerator. It started with a 10-cm radius cylinder at the cathode end plate and tapered off to 1-cm radius at the A-K gap of a magnetically immersed foilless diode (Figure 2). Seven conical tapers were utilized along with eight cylindrical sections and an equal number of flex-adjusting, double washer sections. The outer shell (anode cylinder) was formed by eight 19-cm inner-radius insulating stacks (feeds) alternating with seven stainless steel cylinders, plus the final anode extension cylinder. The cathode electrode (Figure 3) was preloaded before insertion into the anode cylinder to compensate for gravitational droop. The final adjustment was made in situ. Because of the large difference in radius between anode and cathode shank, precise alignment and centering of the cathode stock inside the anode cylinder was not very critical since the electrical potential is a logarithmic function of the radii.

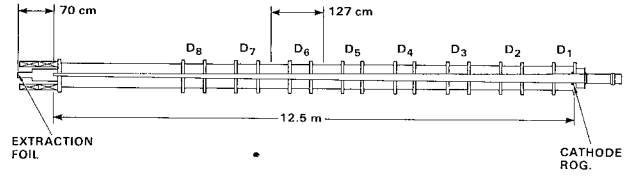


Fig. 2: RADLAC II/SMILE configuration.

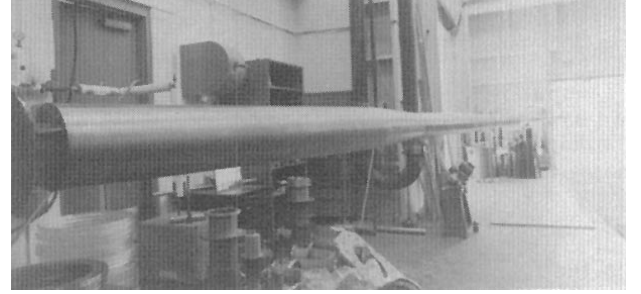


Fig. 3: SMILE cathode electrode before insertion into the anode cylinder.

The magnetically-immersed foilless diode design (Figure 4) was similar to that of the IBEX accelerator¹¹ and actually utilized the same pancake coil assembly. The anode extension cylinder made it possible to locate the diode outside of the water tank and greatly facilitated operations and beam parameters evaluation.

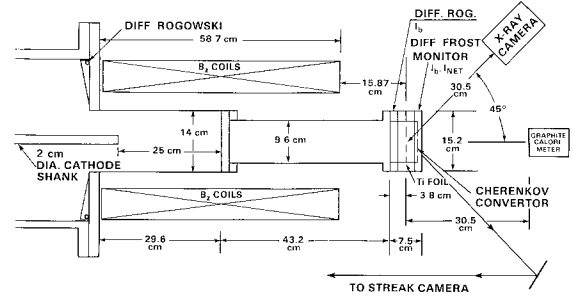


Fig. 4: Schematic diagram of the immersed foilless diode with beam diagnostics.

The main differences between HERMES III⁷ and SMILE designs are the current or operating impedances and the length of the voltage feeds. The RADLAC II feeds were 50-cm long while those of HERMES III are only 3.8 cm. This made SMILE almost a "continuous" adder, the first of its kind. Another first is that SMILE was the highest impedance 16-MV MITL voltage adder. The final operating impedance is 150 ohm versus 30 ohm of HERMES III. These differences made the design, construction and operation of the SMILE adder very challenging.

Simulation Results

The design parameters of Table I were validated with a number of MAGIC simulations. The calculated impedances agreed with the minimum parapotential theory⁸ within 10%. Figure 5 compares the voltage input of each feed with the MAGIC simulated total output voltage applied at the A-K gap of the electron diode.

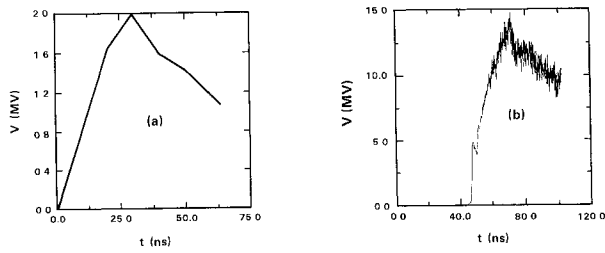


Fig. 5: Time dependence of RADLAC/SMILE input voltage (a) and combined 8-feed voltage output at the A-K gap of the foilless diode (b).

Computer-generated movies of SMILE simulations show that we have self-magnetic insulation during a large part of the input voltage waveform. There are some electron losses at the beginning and at the end of the voltage pulse. This is to be expected since self-limited magnetic insulation is established by driving some electron current to the anode wall during the rise time of the voltage pulse. The losses during the fall time are due to the fact that the current drops below the minimum current I_0 and the line loses self-magnetic insulation. In addition, some of the electrons at the peak of the voltage pulse are lost to the anode cylinder due to the extreme triangular shape of the voltage pulse produced by the RADLAC II pulse forming lines [Figure 5(a)]. This results in the reduction of voltage available at the diode A-K gap by approximately 2 MV [Figure 5(b)]. Figure 6 shows an electron map at 75 ns following the arrival of the voltage pulse at the first feed ($t = 0$). The line is magnetically insulated. The losses near the cathode tip are due to the radial component B_r of the applied magnetic field of the immersed foilless diode. They occur at the point where the self field B_θ becomes equal to the B_r component of the applied field at the immersed foilless diode.

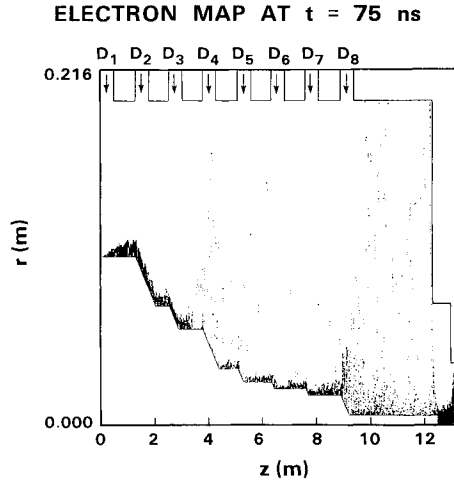


Fig. 6: Electron map for SMILE obtained with MAGIC PIC code at 75 ns after energizing the first insulating Stack D_1 .

The immersed foilless diode is not adequately resolved in Figure 6 because of the actual length of the simulated structure (12.5 m) and the size of the numerical grids. However, using as an input the voltage waveform obtained from simulations like the one in Figure 5(b), we studied in separate simulations the quality of the produced beam.

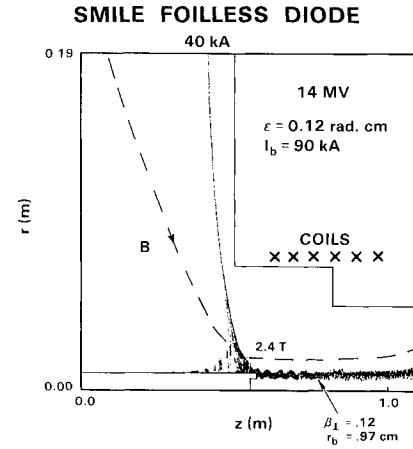


Fig. 7: MAGIC simulation of a SMILE foilless diode configuration.

A number of electron diode options were analyzed including foil diodes, apertured diodes¹² and magnetically immersed foilless diodes. Figure 7 shows that we can produce high quality electron beams with very small transverse velocity components β_\perp . Actually, the experimental results suggest even lower transverse velocities. It appears that coupling an MITL line with a magnetically immersed foilless diode eliminates most of the outer edge, higher temperature sheath electrons that follow the central conductor. The radial magnetic field produced by the short solenoid (Figure 4) of the foilless diode acts as a filter directing the hot sheath electrons to the anode wall. Extensive foilless diode simulations demonstrated that both temperature and current decrease with an increase in the B_z field. The A-K gap affects the produced current to a certain extent. However, when it becomes as large as in Figure 4 (25 cm), it becomes ineffective in fine tuning the beam.

Experimental Measurements

Figure 4 is a schematic diagram of the immersed foilless diode and the diagnostics utilized to evaluate the beam parameters. The beam current was measured by the two differential Rogowski coils located at the anode plane and near the exit foil. The beam energy was evaluated from the voltages measured along each of the eight feeds. Eight resistive monitors were used. The net accelerating voltage across the A-K gap of the diode was assumed to be the sum of the feed voltages shifted in time to coincide with the passage of the current pulse through each feed.

The beam annulus, radius and thickness were measured utilizing an integrated x-ray pinhole camera and beam witness foils (Figure 4). From the annulus thickness W we can in a straightforward manner calculate the β_\perp of the beam if the energy γ , magnetic field B_z , and cathode tip radius and annulus thickness α are known:

$$\beta_\perp = (W - \alpha) [cm] B_z [kG] / 3.4\gamma \quad (4)$$

A few measurements were done with the extraction and radiochromic foil located inside the axially uniform guiding magnetic field. However because of frequent foil blow-ups and vacuum losses, the beam was often extracted at approximately half the field, the extraction foil being located at the diverging fringing field of the solenoidal magnet. The observed beam radius at the foil provides an independent estimate of the magnetic field at extraction assuming adiabatic beam expansion. Experimental measurements of beam annulus thickness and radius similar to those of Figure 8 gave beam transverse velocity components $\beta_\perp \leq 0.1$ with the average value being closer to $\beta_\perp = 0.05$.

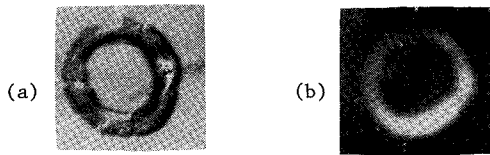


Fig. 8: (a) Imprint of the beam on the witness foil.
(b) X-ray pinhole photograph of the beam at extraction. The cross is an alignment fiducial. The non-uniformity of the annulus is mainly due to x-ray obstruction by the beam line hardware.

The SMILE operated reliably, consistently producing high quality, high current electron beams with parameters repeating themselves from shot to shot. From the first shot we extracted thin annular beams with radius $r_b \leq 2$ cm into full pressure air. The voltage and current waveforms were similar to those of the first SMILE shot shown in Figure 9. The observed beam radii and currents are in good agreement with simulation; however, the beam transverse temperatures appear to be smaller by a factor of two. One plausible explanation for the obtained low temperature beam is that all the sheath electrons of large radius escape to the anode following the radial magnetic flux lines of the applied B_z field.

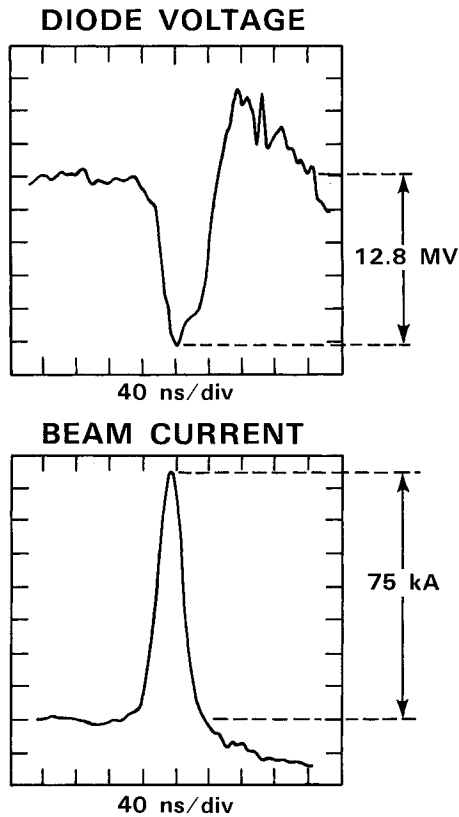


Fig. 9: Voltage and current waveforms of the SMILE magnetically insulated diode. At this first shot, the Marx generators were charged to 90% of the maximum operating voltage.

Conclusions

We designed and installed into the RADLAC II accelerator a self-magnetically insulated transmission line SMILE. The coaxial transmission line replaced the original beam line that had solenoidal magnets and accelerating gaps and performed the voltage addition along the long cathode shank. It utilized the same pulse forming network and accelerating cavities (feeds). The total voltage was applied at the A-K gap of a magnetically immersed foilless diode located at the end of the coaxial line outside the water tank.

SMILE operation was reliable and reproducible, consistently generated beams with low transverse velocities (≤ 0.1) and small radii (~ 1 cm).

The beam current could be varied between 50 and 100 kA by changing diode parameters such as A-K gap and magnetic field strength. The observed beam radius and current were in good agreement with diode numerical simulations. However, the beam temperatures were lower by almost a factor of two. SMILE made RADLAC II a reliable device for high current, high energy electron beam production and physics studies of beam propagation in air.

References

1. R. B. Miller, et al. J. Appl. Phys. **51**, 3506 (1980).
2. G. Yonas, Private Communication (1981).
3. J. H. Creedon, J. Appl. Phys. **48**, No. 3, 1070 (1977).
4. M. G. Mazarakis, et al., 1989 IEEE Particle Accelerator Conference, Chicago, IL, p. 1002 (March 20-23, 1989) 89CH2669-0.
5. M. G. Mazarakis, et al., Bull. Am. Phys. Soc. **35**, No. 4, 931 (1990).
6. J. J. Ramirez, et al., Proc. 5th International IEEE Pulsed Power Conference, Arlington, VA, p. 143 (June 10-12, 1985).
7. R. C. Pate, et al., Proc. 6th International IEEE Pulsed Power Conference, Arlington, VA, p. 478 (June 29-July 1, 1987).
8. D. L. Johnson, et al., Bull. Am. Phys. Soc. **35**, No. 4, 955 (1990).
9. J. Corley, et al., This Conference.
10. T. W. L. Stanford, et al., J. Appl. Phys. **63** (3), 681 (1988).
11. M. G. Mazarakis, et al., J. Appl. Phys. **62**, 4024 (1987).
12. J. W. Poukey, et al., Proc. 1990 Linear Accelerator Conference, Albuquerque, NM, LA-12004-C, p. 608 (Sept. 10-14, 1990).